Original scientific paper
https://doi.org/10.33180/InfMIDEM2024.103

Informacije MIDEM
Journal of Microelectronics,
Electronic Components and Materials
Vol. 54, No. 1(2024), 25 – 38

# *Examination of Resistive Switching Energy of Some Nonlinear Dopant Drift Memristor Models*

*Rabia Korkmaz Tan[1], Oya Mert[2], Resat Mutlu[3]*

*[1]Department of Computer Engineering, Çorlu Faculty of Engineering, Tekirdağ Namık Kemal University, Çorlu, Tekirdağ, Turkey*
*[2]Department of Mathematics, Faculty of Arts and Sciences, Tekirdağ Namık Kemal University, Tekirdağ, Turkey*
*[3]Department of Electronics and Communication Engineering, Çorlu Faculty of Engineering, Tekirdağ Namık Kemal University, Çorlu, Tekirdağ, Turkey*

**Abstract:** In the literature, there are memristor models based on nonlinear drift mechanisms and window functions. Memristors can be employed to model resistive memories. When the resistance of a memristor undergoes a transition from its lowest value to its highest value, or vice versa, this phenomenon is referred to as resistive or memristive switching. The energy required for this transition holds particular importance, especially in the context of resistive computer memory and digital logic applications. Experimental measurements can be used to determine the resistive switching energy, and it should also be possible to calculate it theoretically based on the parameters of the memristor model utilized. Recently, the resistive switching times of some of the nonlinear dopant drift memristor models have been examined analytically considering especially their memory and digital circuit applications. In the literature, to the best of our knowledge, the resistive switching energy of the nonlinear dopant drift memristor models has not been calculated and examined in detail. In this study, the memristive switching energy of some of the well-known memristor models using a window function is calculated and found to be infinite. This is not feasible according to the experiments in which a finite resistive switching energy is consumed. The criterion that a memristor must have a finite resistive energy is also presented in this study. The results and the criterion for the resistive switching energy presented in this paper can be utilized to build more realistic memristor models in the future.

**Keywords:** Memristor, memristor models, resistive memories, window function, memristive switching, resistive switching

# *Preučevanje upornostne preklopne energije nekaterih modelov memristorjev z nelinearnim odstopanjem dopanta*

**Izvleček:** V literaturi obstajajo modeli memristorjev, ki temeljijo na nelinearnih mehanizmih odstopanj in okenskih funkcijah. Memristorji se lahko uporabijo za modeliranje uporovnih pomnilnikov. Ko upornost memristorja preide iz najnižje vrednosti v najvišjo ali obratno, se ta pojav imenuje uporovno ali memristivno preklapljanje. Energija, ki je potrebna za ta prehod, je še posebej pomembna, zlasti v kontekstu uporovnega računalniškega pomnilnika in digitalne logike. Za določitev energije uporovnega preklopa se lahko uporabijo eksperimentalne meritve, prav tako pa jo je mogoče teoretično izračunati na podlagi parametrov uporabljenega modela memristorja. Nedavno so bili analitično preučeni uporovni preklopni časi nekaterih nelinearnih modelov memristorjev z odstopanjem dopanta, pri čemer so bile upoštevane zlasti njihove aplikacije za pomnilnike in digitalna vezja. V literaturi, kolikor nam je znano, uporovna preklopna energija memristorskih modelov z nelinearnim odstopanjem dopanta ni bila izračunana in podrobno preučena. V tej študiji je izračunana energija memristivnega preklopa nekaterih znanih modelov memristorjev z uporabo okenske funkcije in ugotovljeno je, da je neskončna. Glede na poskuse, pri katerih se porabi končna uporovna preklopna energija, to ni izvedljivo. V tej študiji je predstavljeno tudi merilo, da mora imeti memristor končno uporovno energijo. Rezultati in merilo za uporovno preklopno energijo, predstavljeni v tem članku, se lahko v prihodnosti uporabijo za izdelavo bolj realističnih modelov memristorjev.

**Ključne besede:** memristor, modeli memristorjev, uporovni pomnilniki, funkcija okna, memristivno preklapljanje, uporovno preklapljanje

** Corresponding Author's e-mail: rmutlu@nku.edu.tr*

How to cite:
R. K. Tan et al., "Examination of Resistive Switching Energy of Some Nonlinear Dopant Drift Memristor Models", Inf. Midem-J. Microelectron. Electron. Compon. Mater., Vol. 54, No. 1(2024), pp. 25–38

## 1 Introduction

In his influential article published in 1971, Dr. Chua introduced the memristor as the novel and fourth passive circuit element, joining the ranks of the resistor, inductor, and capacitor [1]. A perfect memristor is a passive circuit element that possesses two terminals and exhibits a nonlinear correlation between magnetic flux and electrical charge. The memristor has a resistance that varies by its charge, known also as memristance, and it also consumes power [1]. In 1976, a class of systems known as memristive systems, possessing properties akin to memristors, was introduced [2]. After nearly four decades after Dr. Chua's initial proposition, a nano-sized TiO2 thin film memristive system developed in Hewlett-Packard (HP) laboratory was demonstrated to possess memristor-like traits similar to those anticipated for its operation [3]. Hence, in 2008, the revelation of a novel nonlinear electronic circuit element, demonstrating memristor-like characteristics within certain operation ranges, captured global attention, leading to a surge in research and exploration of memristors and memristive systems [4-9]. Memristors have been explored for their non-volatile memory capabilities and dynamic load applications, as discussed in [4]. Memory phenomena are frequently observed in nanoscale devices, and certain effects can be effectively modeled using memristors [5]. The resistive memories, which are popular study areas nowadays, also behave as memristors and are regarded as memristors by Chua [6]. Domaradzki et al. provide a review of the applications of memristors in circuit design and computer technology [7]. The usage of memristors in various applications, such as memory, analog, logic, and neuromorphic circuits, is investigated in [8]. Memristor-based circuit applications encompass a variety of electronic circuits, including amplifiers [9, 10], oscillators [11], filters [11, 12], computer memories [6] and artificial neural network circuits [13]. A significant portion of memristor research has been devoted to modeling this novel circuit element. The pioneering and most basic physical model of a memristor was initially introduced in [3]. Williams and colleagues proposed the HP memristor model, assuming that the ion drift speed inside the memristor is directly proportional to the memristor current and remains uniform throughout the memristor. While the model is straightforward to comprehend, it incorporates a linear dopant drift and is considered obsolete now. Due to the discrepancy with the actual heterogeneous dispersion of ions, researchers have developed memristor models with nonlinear ion drift speeds, utilizing window functions to address this issue [3, 14-18]. The models presented in [14-16] face challenges related to boundary lock issues. To address this problem, researchers have developed polarity-dependent window functions, as described in [15-17].

Chua has classified resistive memories as memristive systems [6]. Even after a memristor is turned off, it retains its last resistance value, and upon repowering, it resumes operation from that resistance value [1, 3, 6]. A memristor does not consume power when its current is zero [6]. This unique characteristic makes Non-Volatile Random-Access Memory (NVRAM) one of the most significant applications of memristive systems [4-8]. ReRAM application of the TiO2-based memristors is reviewed in [19]. Moreover, there is potential to develop high-density memristor-based Static Random-Access Memories (SRAMs) that consume low-power [20]. The initial discovery of the ReRAM structure involved nickel oxide (NiO) in 1964 [21]. Since then, various materials have been identified as suitable candidates for creating resistive memories [5, 7, 22-25]. The following examples are only a few of these materials. Silicon oxide has been utilized in the fabrication of resistive memories [22]. Moreover, the examination of conducting nanofilaments within a Pt/TiO2/Pt system during resistive switching has been investigated in [23]. [24] explores the memristive switching mechanism in metal/oxide/metal nanodevices. Furthermore, [25] presents a comprehensive examination of both bipolar and unipolar operations in Resistive Random Access Memory (ReRAM). Waser et al. suggest a broad classification into thermal, electrical, or ion-migration-induced switching mechanisms [26]. Choi et al. conducted atomic force microscopy studies using different vacuum conditions, showing a strong correlation between resistance switching and the creation and elimination of conducting spots [27]. The experimental findings presented in [28] demonstrate that the introduction of Si or Al implantation into HfO2 films leads to lower electroforming voltages and enhances the reproducibility of resistive switching. Sivkov et al. investigated the impact of thickness variation and electrode size on the resistive switching properties of ZrO2 [29]. Linn et al. investigated the resistive switching properties of the complementary resistive switches (CRS) and explored their potential utilization in passive nano crossbar memories to achieve power consumption reduction [30]. Rosezin et al. showcased the vertical integration of Complementary resistive switch cells utilizing Cu/SiO2/Pt bipolar resistive switches [31]. By employing CRS-based memristors, 3D stacking crossbar memories experience reduced leakage current [32]. However, it is important to note that such CRS-based memories may require reconstructive circuits to rewrite the deleted information during reading [33].

Memristive materials find application in digital circuitry as well. The literature also explores various memristor-based digital circuits, including reconfigurable logic circuits, flip-flops, latches, and more [34-40]. Memristor-based programmable logic circuits can be developed

[34]. The memristor-based flip-flop circuits possess nonvolatile characteristics and operate with low power consumption [35-37]. Memristors make the production of reconfigurable logic gates and devices possible [38, 39]. However, it is important to consider that implementing memristor-based logic and memory circuits might necessitate the use of adaptive writing circuits [33-40]. Vourkas et al. provide an overview of the design of memristor-based logic circuits [40].

The phenomenon in which a memristor's resistance transitions from $R_{on}$ to $R_{off}$ or from $R_{off}$ to $R_{on}$ when subjected to an applied voltage is referred to as 'memristive switching' or 'resistive switching' [41]. The duration needed for this process is referred to as the "memristive switching time" or "resistive switching time". The writing or erasing of memristor-based memories, as well as other memristor-based digital applications mentioned earlier, rely on the occurrence of memristive switching. This emphasizes the significance of the memristive or resistive switching time as a vital parameter in evaluating the effectiveness of memristor-based computer memories and memristor-based digital circuits [6, 8, 18, 30, 33, 41, 42]. Wang et al. have explored the conceptual and experimental aspects of memristive switching time, employing a piecewise linear charge-flux characteristic [41]. This time value may vary depending on the direction of the memristor current [15, 17, 18]. In [43], researchers have analyzed and conducted experimental investigations to explore the consequences of delayed memristive switching in memristor-based artificial neural networks. The research presented in [44, 45] involves the calculation of the memristive switching time using the HP memristor model. [46] proposes that memristive switching can be utilized for calculating the memristance function. In [18], the resistive switching times of the memristor models presented in [3, 14-17] are calculated using their respective window functions for both polarities, the computation of complex integrals for determining the resistive switching times is performed using the Wolfram Alpha program, and it is observed that the integrals diverge except the HP memristor model. The solutions of these integrals are analyzed and interpreted, leading to a diagnosis of the boundary unreachability problem in these models with an infinite switching time and the proposal of a new memristor model that provides a finite switching time [18].

In literature, different types of memories are compared for their power consumption [20, 30-32, 39, 47-49]. However, there are only a few papers regarding memristor power consumption [50-53]. In [50], an AC power formula for memristors under small signal excitation is given. In [51], the power consumption of memristor-based relaxation oscillators is examined with the instantaneous memristor power formula. In [39], it is shown that the tolerances of the memristors result in a different switching time for each memristor and, therefore, a different energy loss for writing and deleting a memristor. The resistive switching energy besides resistive switching time is an important parameter in memristor-based memory and digital applications such as flip-flops, logic gates, etc. The required resistive switching energy should be calculatable with the parameters of the memristor model used to model the device. The paper aims to examine the resistive switching energy of some of the well-known memristor models. In this paper, first, the resistive or memristive switching energy formula for the nonlinear drift speed memristor models is derived, and, then, the memristive switching energy of the memristor models given in [3, 14-18] is tried to be calculated with their window functions considering both polarities. The WolframAlpha program is used to solve the definite integrals of the resistive switching energy. Some of the definite integrals are shown to diverge. The interpretation of the results is done.

This paper is structured as follows. In the second section, the nonlinear dopant drift memristor model and the window functions used in this study are summarized. In the third section, the derivation of the integral formula to calculate the memristive switching energy considering the memristor polarity is made. Analytical solutions of the switching times of the nonlinear dopant drift memristor models are sought in the fourth section. The paper is finished with the conclusion section.

## 2 Memristor models and their window functions

This section provides a brief explanation of the memristor models employed in this study. A memristor, which is also a memristive system [2], is described as an (ideal) device where the charge of the memristor serves as the system's state variable. Nevertheless, the present-day terminology refers to thin-film systems, which fall under the category of memristive systems, as memristors [54]. One particular memristor model, characterized by nonlinear dopant drift, is represented by the following equations:

$$v(t) = R(x).i(t). \tag{1}$$

$$dx/dt = \mu_v \frac{R_{on}}{D^2}.i(t) f(x,i). \tag{2}$$

where $i(t)$, $v(t)$, $R(x)$, $R_{on}$, $x(t)$ and $f(x, i)$ are the current, voltage, resistance, minimum resistance, state variable,

and polarity-dependent window function of the memristor, respectively, *D* is the total length of the TiOx region, and $\mu_g$ is the dopant mobility of the TiO2 region.

The state variable of the memristor, which represents its normalized oxidized length, can be mathematically expressed as

$$x = w/D \tag{3}$$

where  denotes its current oxidized length.

To determine the rate of drift speed in this memristor model, a window function is introduced, which involves multiplying the memristor current according to equation (2) [3, 14-18]. The memristor memristance or resistance is expressed as

$$R(x) = R_{on}\, x + R_{off}\,(1-x) = R_{off} - (R_{off} - R_{on})\, x \tag{4}$$

Based on the model presented in [3] a memristor's resistance varies within the range of its minimum value, $R_{on}$, to its maximum value, $R_{off}$. Consequently, the following statement always holds for the resistance of a memristor:

$$R_{off} \geq R(x) \geq R_{on} \tag{5}$$

This research utilizes memristor models proposed by Strukov [3] Joglekar [14], Biolek [15] Prodromakis [16] Zha [17], Mutlu-Kumru [18]. A comprehensive overview of the memristor models employed in this study is available in [55]. These models are characterized by window functions, which act as indicators of the degree to which a memristor emulates an ideal memristor [15]. The corresponding window functions are detailed in Table 1.

While the literature represents polarity-dependent window functions as *f(x),* in this study, they are represented as *f(x, i)* to include the polarity variable.

The resistance value or memristive state variable of these memristors begins to change only when both their window function and current are not equal to zero. The window functions described in [14, 16], which exhibit zero dopant speeds at the boundaries of the memristive layer, face an issue known as the boundary lock problem: at $x = 0$ and $x = 1$, their resistance value, memristive state-variable, or window function *f(x)* remains unchanged regardless of the value of current flowing. The models presented in [15, 17-18] do not experience these problems. All the window functions listed in Table 1 are phenomenal functions.

The experimental data might lead to the development of more realistic window functions with improved accuracy in the future. The window function of the HP model is regarded as being equal to one [3]. The "stp()" function in Table 1 represents the unit step function and is defined as follows.

$$stp(i) = \begin{cases} 1 & , \quad i \geq 0 \\ 0 & , \quad i < 0 \end{cases} \tag{6}$$

Comparisons of the mentioned window functions, whose resistive switching time is examined in [18] are given in Table 2.

The Strukov model is characterized by a non-scalable quadratic window function and suffers from a boundary lock issue. This means that once the boundary is reached, the regions become fixed at the boundaries, causing the model to function like a resistor. Even changing the polarity cannot resolve the problem because $f(0) = f(1) = 0$. The window function of the Joglekar model incorporates a shaping parameter (*p*), which allows for modifications to its shape. However, it also exhibits a boundary lock issue. On the other hand, the Biolek model features a current polarity-dependent window function.

When the current of the Biolek memristor model is positive and its window function at $x = 1$ is 0, this causes the memristor to act as a linear time-invariant (LTI) resistor. However, when the current of the Biolek memristor model is negative and its window function at $x = 1$ is 1, this results in a change in the memristor's resistance. On the other hand, when the current of the Biolek memristor model is negative and its window function at $x = 0$ is 0, the memristor behaves as a resistor. But, when the current of the Biolek memristor model is positive and its window function at $x = 0$ is 1, this leads to a variation in the memristor's resistance. Altering the current polarity in the model leads to a change in its resistance, thereby eliminating any boundary lock issues. Nevertheless, it is important to note that the model lacks scalability.

The Prodromakis model exhibits a boundary lock problem, but its window function can be scaled using the parameter j. Moreover, the Zha model integrates the polarity dependency of Biolek's window function with the scalability of Prodromakis' window function.

**Table 1:** The memristor window functions used in this study

| The model | Its window function (f(x) or f(x, i)) |
|---|---|
| HP | $f(x)=1$ |
| Strukov | $f(x)=x-x^2$ |
| Joglekar | $f(x)=1-(2x-1)^{2p}$ |
| Biolek | $f(x,i)=1-\left(x-stp(-i(t))\right)^{2p}$ |
| Prodromakis | $f(x)=j\left(1-\left((x-0.5)^2+0.75\right)^p\right)$ |
| Zha | $f(x,i)=j\left(1-\left(0.25\left(x-stp(-i)\right)^2+0.75\right)^p\right)$ |
| Mutlu-Kumru | $f(x,i)m_1\sqrt[x]{1-x}.stp(i)+m_2\sqrt[x]{x}.stp(-i)$ |

**Table 2:** Comparison of the memristor window functions used in this study

| Window functions | Strukov | Joglekar | Biolek | Prodromakis | Zha | Mutlu-Kumru |
|---|---|---|---|---|---|---|
| Variables of the window function | x | x | x, i | x | x, i | x, i |
| Formability | No | Yes | Yes | Yes | Yes | Yes |
| Formability parameter | - | p | p | p | p | n |
| Scalability | No | No | No | Yes | Yes | Yes |
| Scalability parameter | - | - | - | j | j | $m_1$, $m_2$ |
| Problem of boundary lock | Yes | Yes | No | Yes | No | No |
| Boundary unreachability | No | No | Yes | No | Yes | No |

The resistive switching times of the memristor models given in Table 3 are calculated for each polarity in [18]. Only, the HP and Mutlu-Kumru Models have given finite resistive switching times values.

## *3 Derivation of resistive switching energy formula of nonlinear dopant drift memristive models*

The circuits, which are shown in Fig. 1, can be used to make the memristive switching occur. The memristor in the circuit in Fig. 1a is forward-biased and a positive DC voltage is applied to it, and the switch is turned on at a time equal to zero. If the memristor resistance is equal to $R_{off}$ at $t = 0$, the memristor resistance falls down from $R_{off}$ to $R_{on}$ in this case. The memristor in the circuit in Fig. 1b is reverse-biased and a negative DC voltage is applied to it, and the switch is turned on at a time equal to zero. If the memristor resistance is equal to $R_{on}$ at $t = 0$, the memristor memristance goes from $R_{on}$ to $R_{off}$ in that case. For polarity dependent memristor models, the memristive or resistive switching Energy must be found for each polarity.

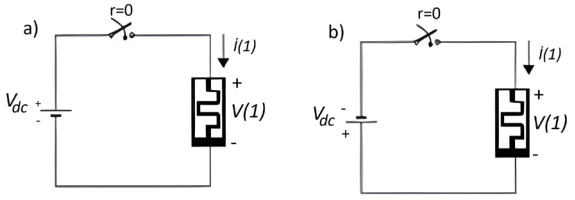


**Figure 1:** The memristor supplied by a) a positive DC voltage source for the forward resistive switching (*x* goes up from 0 to 1) and b) a negative DC voltage source for the reverse resistive switching (*x* goes down from 1 to 0)

**Table 3:** The resistive switching times of the memristor models

| The model | Its resistive switching time in the forward direction | Its resistive switching time in the reverse direction |
|---|---|---|
| HP | $\frac{D^2\left(R_{on}+R_{off}\right)}{2\mu_V R_{on}V_{dc}}$ | $\frac{D^2\left(R_{on}+R_{off}\right)}{2\mu_V R_{on}V_{dc}}$ |
| Strukov | $\infty$ | $\infty$ |
| Joglekar | $\infty$ | $\infty$ |
| Biolek | $\infty$ | $\infty$ |
| Prodromakis | $\infty$ | $\infty$ |
| Zha | $\infty$ | $\infty$ |
| Mutlu-Kumru | $\left(\frac{R_{on}-R_{off}}{V_{dc}Km_1}\right)\left(\frac{n}{2n-1}\right)+\frac{R_{off}}{V_{dc}Km_1}\left(\frac{n}{n-1}\right)$ | $\frac{1}{V_{dc}K}\left(\frac{R_{on}-R_{off}}{m_2}\left(\frac{n}{2n-1}\right)+\frac{R_{off}}{m_2}\left(\frac{n}{n-1}\right)\right)$ |

Considering the nonlinear memristor models explained before, the memristive switching energy can be calculated as follows. The current of a forward-biased memristor supplied with the constant voltage $V_{dc}$ is

$$i(t)=\frac{v(t)}{R(x)}=\frac{V_{dc}}{R(x)}. \tag{7}$$

The power of the memristor is

$$p(t)=v(t)i(t)=v(t)\frac{v(t)}{R(x)}=\frac{(V_{dc})^2}{R(x)}. \tag{8}$$

For a forward-biased memristor, the energy consumption of the memristor, in which *x(t)* rises from 0 to 1, is calculated as

$$E_{SWP}=\int_0^{\tau_{SWP}}p(t)\,dt=\int_0^{\tau_{SWP}}\frac{(V_{dc})^2}{R(x)}dt \tag{9}$$

The derivative of the state variable of the memristive models can be written as

$$\frac{dx}{dt}=\frac{\mu_V R_{on}}{D^2}i(t)f(x)=\frac{\mu_V R_{on}V_{dc}f(x)}{D^2R(x)} \tag{10}$$

By rearranging (10),

$$dt=\frac{D^2R(x)\,dx}{\mu_V R_{on}V_{dc}f(x)} \tag{11}$$

During the forward resistive switching: at $t=\tau_{SWP}$, $x(\tau_{SWP})=1$ and, at $t=0$, $x(0)=0$. Submitting Eq. (11) into Eq. (9):

$$\begin{aligned}E_{SWP}&=\int_0^1\frac{(V_{dc})^2}{R(x)}\frac{D^2R(x)\,dx}{\mu_V R_{on}V_{dc}f(x)}=\frac{V_{dc}D^2}{\mu_V R_{on}}\int_0^1\frac{dx}{f(x)}.\\&=\frac{V_{dc}D^2}{\mu_V R_{on}}\int_0^1\frac{dx}{f(x)}.\end{aligned} \tag{12}$$

The energy or the integral in Eq. (12) depends on the window function of the forward-biased memristor. Assuming that, after the forward resistive switching occurs, for a short time, the device continuous on drawing current since the applied pulse width is wider than its forward switching time ($\tau_{SWP}\le T_p$), an additional conduction loss occurs. It can be calculated as:

$$E_{CP}=\int_{\tau_{SWP}}^{T_P}p(t)\,dt=\int_{\tau_{SWP}}^{T_P}\frac{(V_{dc})^2}{R_{on}}dt=\frac{(V_{dc})^2}{R_{on}}(T_P-\tau_{SWP}) \tag{13}$$

Then, the total loss in this case can be found as:

$$E_P=E_{SWP}+E_{CP} \tag{14}$$

For a reverse-biased memristor, the switching voltage is negative and equal *to* $-V_{dc}$, the energy consumption of the memristor, in which *x(t)* falls down from 1 to 0, is calculated as

$$E_{SWN}=\int_0^{\tau_{SWN}}p(t)\,dt=\int_0^{\tau_{SWN}}\frac{(V_{dc})^2}{R(x)}dt \tag{15}$$

The energy or the integral in Eq. (12) depends on the window function of the forward-biased memristor.

During the reverse resistive switching: at $t=\tau_{SWN}$, $x(\tau_{SWN})=0$ and, at $t=0$, $x(0)=1$. Submitting Eq. (11) into Eq. (15):

$$\begin{aligned}E_{SWN}&=\int_1^0\frac{(V_{dc})^2}{R(x)}\frac{D^2R(x)\,dx}{\mu_V R_{on}(-V_{dc})f(x)}=\\&=-\frac{V_{dc}D^2}{\mu_V R_{on}}\int_1^0\frac{dx}{f(x)}=\frac{V_{dc}D^2}{\mu_V R_{on}}\int_0^1\frac{dx}{f(x)}.\end{aligned} \tag{16}$$

Eq. (16) is the same as Eq. (13) but the window function for the correct polarity should be utilized to calculate the switching energy.

The energy or the integral in Eq. (16) depends on the window function of the reverse-biased memristor. Assuming that, after the reverse resistive switching occurs, for a short time the device continuous on drawing current since the applied pulse width is wider than its reverse switching time ($\tau_{SWN}\le T_p$), an additional conduction loss occurs. It can be calculated as:

$$E_{CN}=\int_{\tau_{SWN}}^{T_P}p(t)\,dt=\int_{\tau_{SWN}}^{T_P}\frac{(-V_{dc})^2}{R_{off}}dt=\frac{(V_{dc})^2}{R_{off}}(T_P-\tau_{SWN}) \tag{17}$$

Then, the total loss can be found as:

$$E_N=E_{SWN}+E_{CN} \tag{18}$$

Considering Eq.s (12) and (16), for a nonlinear dopant drift memristor model, the resistive switching energy is proportional to the DC voltage applied, and the memristor parameters, D, $\mu_v$, and $R_{on}$, the switching voltage $V_{dc}$ define the resistive switching energy, the lower the minimum resistance of the memristor, the higher the resistive switching energy. However, the conduction loss of the memristor depends on only $R_{on}$ for the forward-biased memristor and $R_{off}$ for the reverse-biased memristor. If a memristor model's window function is not dependent on polarity, the resistive switching energy for each polarity is the same:

$$E_{SWP} = E_{SWN} \tag{19}$$

## 4 Examination of resistive switching energy of nonlinear dopant drift memristive models

In this section, the switching energy of the examined memristor models can be found using the derived equations.

### 4.1 Resistive switching energy of the HP memristor model

The HP memristor model is the first memristor model given in the literature [3]. It is the simpler than the other memristor models examined in this study [18]. In this model, it is assumed that the linear dopant drift exists in the memristive element [3]. The window function of the HP memristor model is equal to one, i.e., f(x) = 1. The resistive switching energy of an HP memristor is calculated as

$$E_{SWP} = \frac{V_{dc} D^2}{\mu_V R_{on}} \int_0^1 \frac{dx}{f(x)} .$$

$$\begin{aligned} E_{SWP} &= \frac{V_{dc} D^2}{\mu_V R_{on}} \int_0^1 \frac{dx}{1} \\ &= \frac{V_{dc} D^2}{\mu_V R_{on}} \int_0^1 dx \\ &= \frac{V_{dc} D^2}{\mu_V R_{on}} \lfloor x \rfloor_0^1 = \frac{V_{dc} D^2}{\mu_V R_{on}} \end{aligned} \tag{20}$$

In [18] it is shown that the resistive switching time of an HP memristor for each polarity is the same. The resistive switching energy of an HP memristor for each polarity is also the same.

### 4.2 Resistive switching energy of the memristor model with Strukov window function

The Strukov window function does not depend on the polarity of the memristor. It is expressed as

$$f(x) = x - x^2 \tag{21}$$

Therefore, its resistive switching energy is the same for each polarity. Its resistive switching energy is found as

$$\begin{aligned} E_{SWP} = E_{SWN} &= \frac{V_{dc} D^2}{\mu_V R_{on}} \int_0^1 \frac{dx}{f(x)} \\ &= \frac{V_{dc} D^2}{\mu_V R_{on}} \int_0^1 \frac{dx}{x - x^2} \\ &= \frac{V_{dc} D^2}{\mu_V R_{on}} \left( \ln|x| - \ln|1-x| \right)_0^1 = \infty \end{aligned} \tag{22}$$

The resistive switching energy of the memristor model is infinite or its integral diverges. This is expected since the model has a boundary lock problem. In [18], its resistive switching time is also found to be infinite. The resistive switching energy is the same for both directions since the Strukov window function is the same for each polarity.

### 4.3 Resistive switching energy of the memristor model with Joglekar window function

Joglekar window function does not depend on the polarity of the memristor either. It is expressed as

$$f(x) = 1 - (2x-1)^{2p} \tag{23}$$

where *p* is a positive integer used to shape the window function.

That is why its resistive switching energy is the same for each polarity of the memristor. Using Wolfram Alpha for the evaluation of the integral, its resistive switching energy is found as

$$\begin{aligned} E_{SWP} &= \frac{V_{dc} D^2}{\mu_V R_{on}} \int_0^1 \frac{dx}{f(x)} . \\ &= \frac{V_{dc} D^2}{\mu_V R_{on}} \int_0^1 \frac{dx}{1-(2x-1)^{2p}} \\ &= \frac{V_{dc} D^2}{\mu_V R_{on}} \left( \frac{1}{2}(2x-1)\, {}_2F_1\left(1, \frac{1}{2p}; 1+\frac{1}{2p}; (2x-1)^{2p}\right)\right)_0^1 \\ &= \left( \frac{1}{2}(1)\, {}_2F_1\left(1, \frac{1}{2p}; 1+\frac{1}{2p}; 1\right) - \frac{1}{2}0\, {}_2F_1\left(1, \frac{1}{2p}; 1+\frac{1}{2p}; 0\right)\right) = \infty \end{aligned} \tag{24}$$

where ${}_2F_1\left(1, \frac{1}{2p}; 1+\frac{1}{2p}; (x)^{2p}\right)$ is the hypergeometric function whose value becomes infinite for x = 1.

The resistive switching energy of the Joglekar memristor model is infinite or its integral diverges. This is expected since the model has a boundary lock problem. The resistive switching energy is the same for both directions since the Joglekar window function is the same for each polarity. The memristive switching time of the memristor model has also been found to be infinite in [18].

*4.4 Resistive switching energy of the memristor model with Biolek window function*

The Biolek window function depends on the current polarity of the memristor. It can be given as

$$f(x)=1-\left(x-stp\left(-i(t)\right)\right)^{2p} \tag{25}$$

That is why its resistive switching energy should be calculated for both polarities. For the reverse-biased memristor, i.e., for $i \le 0$, using WolframAlpha integral calculator, its resistive switching energy is found as

$$\begin{aligned} E_{SWN} &= \frac{V_{dc}D^2}{\mu_V R_{on}}\int_0^1 \frac{dx}{1-(x-1)^{2p}} \cdot \\ &= \frac{V_{dc}D^2}{\mu_V R_{on}}\left((x-1)\,{}_2F_1\left(1,\frac{1}{2p};1+\frac{1}{2p};(x-1)^{2p}\right)\Big|_0^1\right)=\infty \end{aligned} \tag{26}$$

For the forward-biased memristor, i.e., for $i > 0$, using Wolfram Alpha integral calculator, its resistive switching energy is found as

$$\begin{aligned} E_{SWP} &= \frac{V_{dc}D^2}{\mu_V R_{on}}\int_0^1 \frac{dx}{f(x)} \cdot \\ E_{SWP} &= \frac{V_{dc}D^2}{\mu_V R_{on}}\int_0^1 \frac{dx}{1-(x)^{2p}} \cdot \end{aligned} \tag{27}$$

$$E_{SWP}=\frac{V_{dc}D^2}{\mu_V R_{on}}\left(x\,{}_2F_1\left(1,\frac{1}{2p};1+\frac{1}{2p};(x)^{2p}\right)\Big|_0^1\right)=\infty \tag{28}$$

The resistive switching energy of the Biolek memristor model is infinite for each polarity. The resistive switching time of the Biolek memristor model has also been found to be infinite in [18] due to having the boundary unreachability problem.

*4.5 Resistive switching energy of the memristor model with Prodromakis window function*

The Prodramakis window function does not depend on the memristor polarity either. It is expressed as

$$f(x)=j\left(1-((x-0,5)^2+0,75)^p\right) \tag{29}$$

Therefore, its resistive switching energy is same for both polarities. Using WolframAlpha integral calculator, it is calculated as

$$E_{SWP}=\frac{V_{dc}D^2}{j\mu_V R_{on}}\int_0^1 \frac{dx}{\left(1-((x-0,5)^2+0,75)^p\right)}=\infty \tag{30}$$

The resistive switching energy of the Prodramakis memristor model is found to be infinite or its integral diverges. This is expected since the model has a boundary lock problem. The resistive switching energy is the same for both directions since the Prodramakis window function is the same for each polarity. The memristive switching time of the memristor model has also been found to be infinite in [18].

*4.6 Resistive switching energy of the memristor model with Zha window function*

The Zha window function depends on the memristor polarity and is expressed as

$$f(x)=j\left(1-\left(0.25\left(x-stp\left(-i\right)\right)^2+0.75\right)^p\right) \tag{31}$$

For the forward-biased memristor, i.e., for $i > 0$, using Wolfram Alpha integral calculator, its resistive switching energy is found as

$$E_{SWP}=\frac{V_{dc}D^2}{j\mu_V R_{on}}\int_0^1 \frac{dx}{\left(1-\left(0.25x^2+0.75\right)^p\right)}=\infty \tag{32}$$

The resistive switching energy of the Zha memristor model is infinite for each polarity. The resistive switching time of the Zha memristor model has also been found to be infinite in [18] due to having the boundary unreachability problem.

*4.7 Calculation of resistive switching energy of the memristor model with Mutlu-Kumru window function*

In [18], a new memristor model without boundary lock and boundary unreachability problems have been proposed. It was the only model besides the HP memristor model whose switching times have been able to be calculated. The Mutlu-Kumru window function also depends on the polarity and is given as

$$f(x,i)=m_1\sqrt[n]{1-x}.stp(i)+m_2\sqrt[n]{x}.stp(-i) \tag{33}$$

The function *f(x, i)* considering the memristor polarity can be expressed as the following piece-wise function:

$$f(x,i)=\begin{cases} m_1\sqrt[n]{1-x}, & i\ge 0 \\ m_2\sqrt[n]{x}, & i<0 \end{cases} \tag{34}$$

where $n$ is the shaping constant, which is a positive number, $m_1$ is the forward-polarity scaling constant, $m_2$ is the reverse-polarity scaling constant direction, $i$ is the memristor current.

The Mutlu-Kumru window function for each polarity is shown in Figure 2. The resistive switching energy of the model should be calculated for both polarities. For the forward-biased memristor, i.e., for $i(t) \geq 0$, using Wolfram Alpha integral calculator, its resistive switching energy is found as

$$E_{SWP} = \frac{V_{dc} D^2}{\mu_V R_{on}} \int_0^1 \frac{dx}{m_1 \sqrt[n]{1-x}} = \frac{V_{dc} D^2}{\mu_V R_{on} m_1} \int_0^1 \frac{dx}{\sqrt[n]{1-x}}$$
$$= \frac{V_{dc} D^2}{\mu_V R_{on} m_1} \left( \frac{(1-x)^{1-\frac{1}{n}}}{1-\frac{1}{n}} \right) 1 0 = \frac{V_{dc} D^2}{\mu_V R_{on} m_1} \left( \frac{n}{n-1} \right) \quad (35)$$

For the reverse-biased memristor, i.e., for i ≤ 0, using Wolfram Alpha integral calculator, its resistive switching energy is found as

$$E_{SWN} = \frac{V_{dc} D^2}{\mu_V R_{on}} \int_0^1 \frac{dx}{m_2 \sqrt[n]{x}} = \frac{V_{dc} D^2}{\mu_V R_{on} m_2} \int_0^1 \frac{dx}{\sqrt[n]{x}}$$
$$= \frac{V_{dc} D^2}{\mu_V R_{on} m_2} \left( \frac{n}{n-1} \right) \quad (36)$$

(a)

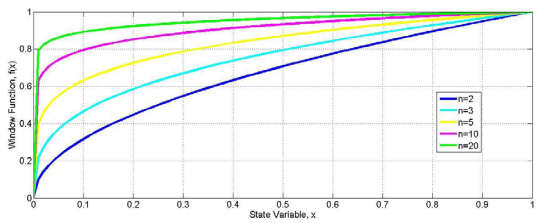


(b)

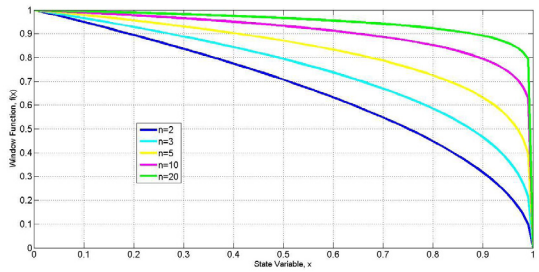


**Figure 2:** The Mutlu-Kumru window function for a) the reverse biased memristor ($i(t) < 0$), various $n$ values, and $m_2 = 1$, and b) for the forward biased memristor ($i(t) > 0$), various $n$ values, and $m_1 = 1$.

From Eq.s (35) and (36), it can be seen that the resistive switching energy converges except for $n = 1$. If $n < 1$, the resistive switching energy of the Mutlu-Kumru memristor model is negative, i.e., the Mutlu-Kumru cannot be used to model a memristor for $n < 1$. If $m_2 = m_1$, the resistive switching energy of the model for each polarity is the same:

$$E_{SWP} = E_{SWN} \quad (37)$$

Also, for the Mutlu-Kumru model, the following relationship can be written as

$$E_{SWN} m_2 = E_{SWP} m_1 \quad (38)$$

In this section, it is also examined how the resistive switching energy varies with respect to $n$, the memristor power exponent, which is used to shape its window function. The reverse resistive switching energy normalized with respect to $\frac{V_{dc} D^2}{\mu_V R_{on} m_2}$ and the forward resistive switching energy normalized with respect to $\frac{V_{dc} D^2}{\mu_V R_{on} m_1}$ as a function of the parameter $n$ is shown in Figure 3. The resistive switching energy asymptotically approaches infinity when n approaches 1. For high values of $n$, Eq.s (35) and (36),

$$E_{SWP} \approx \frac{V_{dc} D^2}{\mu_V R_{on} m_1} \quad (39)$$

and

$$E_{SWN} \approx \frac{V_{dc} D^2}{\mu_V R_{on} m_2} \quad (40)$$

For high values of $n$, Eq.s (40) and (41) become equal to Eq. (11), i.e., the Mutlu-Kumru model turns into the HP memristor model.

In [18], for the reverse-biased memristor, the resistive switching time is given as

$$\tau_{SWN} = \frac{1}{V_{dc} K} \left( \frac{R_{on} - R_{off}}{m_2} \left( \frac{n}{2n-1} \right) + \frac{R_{off}}{m_2} \left( \frac{n}{n-1} \right) \right) \quad (41)$$

In [18], for the forward-biased memristor, the resistive switching time is given as

$$\tau_{SWP} = \left( \frac{R_{on} - R_{off}}{V_{dc} K m_1} \right) \left( \frac{n}{2n-1} \right) + \frac{R_{off}}{V_{dc} K m_1} \left( \frac{n}{n-1} \right) \quad (42)$$

From Eq.s (42) and (43), it can be seen that the switching time converges except for $n = \frac{1}{2}$ and $n = 1$. These two cases have not been reported in [18]:

- If $m_2 = m_1$, the resistive switching times of the Mutlu-Kumru model for each polarity is found as the same.
- If $n < 1$, the resistive switching times of the Mutlu-Kumru is negative, i.e., the Mutlu-Kumru is invalid for $n < 1$.

Also, for the Mutlu-Kumru model, the following relationship can be written as

$$\tau_{SWN} m_2 = \tau_{SWP} m_1 \tag{43}$$

Considering Eq.s (38) and (43),

$$\frac{E_{SWN}}{\tau_{SWN}} = \frac{E_{SWP}}{\tau_{SWP}} \tag{44}$$

(a)

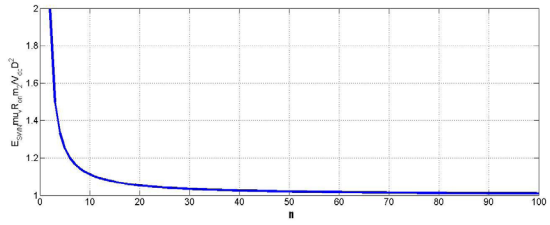

(b)

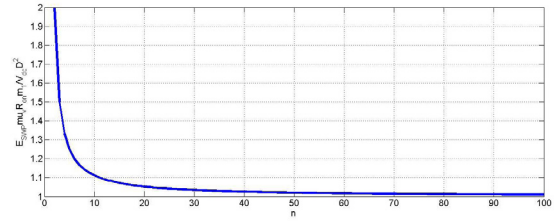

**Figure 3:** The normalized resistive switching energy of the Mutlu-Kumru memristor model with respect to the parameter n for a) the reverse biased memristor (*i(t)* < 0) and b) the forward biased memristor (*i(t)* > 0).

For *i(t)* > 0, the resistive switching time of the Mutlu-Kumru model can also be written as

$$\tau_{SWP} = \left( \frac{R_{on} - R_{off}}{V_{dc} K m_1} \left( \frac{1}{2 - \frac{1}{n}} \right) + \frac{R_{off}}{V_{dc} K m_1} \left( \frac{1}{1 - \frac{1}{n}} \right) \right) \tag{45}$$

For *i(t)* > 0, using the resistive switching energy, the shaping factor of the Mutlu-Kumru model can be found as

$$n = \frac{E_{SWP} \mu_V R_{on} m_1}{E_{SWP} \mu_V R_{on} m_1 - V_{dc} D^2} \tag{46}$$

By summitting (46) into Eq. (45), the relationship between the resistive switching energy and the resistive switching time for the forward-biased memristor is found as

$$\tau_{SWP} = \frac{R_{on} - R_{off}}{V_{dc} K m_1} \left( \frac{1}{2 - \frac{E_{SWP} \mu_V R_{on} m_1 - V_{dc} D^2}{E_{SWP} \mu_V R_{on} m_1}} \right) + \frac{R_{off}}{V_{dc} K m_1} \left( \frac{1}{1 - \frac{E_{SWP} \mu_V R_{on} m_1 - V_{dc} D^2}{E_{SWP} \mu_V R_{on} m_1}} \right) \tag{47}$$

For *i(t)* ≤ 0, the resistive switching time of the Mutlu-Kumru model can also be written as

$$\tau_{SWN} = \frac{1}{V_{dc} K} \left( \frac{R_{on} - R_{off}}{m_2} \left( \frac{1}{2 - \frac{1}{n}} \right) + \frac{R_{off}}{m_2} \left( \frac{1}{1 - \frac{1}{n}} \right) \right) \tag{48}$$

For *i(t)* ≤ 0, using the resistive switching energy, the shaping factor of the Mutlu-Kumru model can be found as

$$n = \frac{E_{SWN} \mu_V R_{on} m_2}{E_{SWN} \mu_V R_{on} m_2 - V_{dc} D^2} \tag{49}$$

By summitting (49) into Eq. (48), the relationship between the resistive switching energy and the resistive switching time for the reverse-biased memristor,

$$\tau_{SWN} = \frac{R_{on} - R_{off}}{V_{dc} K m_2} \left( \frac{1}{2 - \frac{E_{SWN} \mu_V R_{on} m_2 - V_{dc} D^2 1}{E_{SWN} \mu_V R_{on} m_2}} \right) + \frac{R_{off}}{V_{dc} K m_2} \left( \frac{1}{1 - \frac{E_{SWN} \mu_V R_{on} m_2 - V_{dc} D^2 1}{E_{SWN} \mu_V R_{on} m_2}} \right) \tag{50}$$

## 5 Conclusion

The switching energy of memristors or resistive memories is an important physical quantity, that needs to be calculated accurately for digital applications. In this study, first, the resistive switching energy formula for the memristor models is derived. Then, the solutions of the definite integrals of the resistive switching energy of the several well-known memristor models with nonlinear dopant drift speed are given using the Wolf-

ram-Alpha integral calculator. In [18], it was shown that some of the memristor models examined could not do memristive switching in a finite time due to the boundary lock and boundary unreachability problems, i.e., the switching times of these models are found to be infinite except the HP model and the proposed (Mutlu-Kumru) memristor model. In this study, it has been shown that the memristor models with the boundary lock and boundary unreachability problems examined in [18] also require infinite energy for the resistive switching to occur. This is not feasible since an infinite amount of energy cannot be supplied with a physical power source and the calculated switching energy also does not match the experimental results in the literature in which the resistive switching occurs with a finite energy [30, 51, 58]. Amongst the examined models, only the HP memristor and the Mutlu-Kumru model need a finite switching energy. The reason for the infinite energy requirement of the memristor models with boundary unreachability problem has been found as the drift velocity of the doped region inside the memristor decreases to very low values as it approaches the boundaries in these models and, therefore, the resistive switching or the total drifting time takes infinite time, which is regarded as a modern Zeno's paradox in [56]. While the extending doped region approaches any of the boundaries under constant voltage, the doped region slows down so much that the switching time becomes infinite, and this results in an infinite energy consumption. It has also been shown that the models which have an infinite switching time [18] also have an infinite switching energy.

The memristor models well-known and commonly used in the literature are not able to do the resistive switching for whatever the switching voltage is. Any memristor model with this problem is not physically correct. Because, according to experimental studies, the ionic memristors can switch in both directions under a constant voltage and their switching energy increases with increasing voltage. If these memristor models' switching is examined with programs such as Spice, LTspice, and Simulink [15-33] it looks like these memristor models can do resistive switching in a finite time and with finite switching energy according to the simulation results. This is because the numerical methods utilized in the simulation of the resistive switching results in an error. Upon analyzing the switching behavior of these memristors using numerical methods, it appears that the doped region within the memristor can reach either of the boundaries, assuming it moves at the average speed calculated in the previous time. However, [18] demonstrates that this is not valid. The discrete nature of numerical methods like Euler or Range-Kutta makes it impossible to accurately calculate the deceleration of the doped region when it approaches any of the memristor boundaries when a memristor model with boundary unreachability problem is used.

In this study, the effect of memristor polarity on the resistive switching energy was also examined, and it has been demonstrated that the switching energy integral diverges for both polarities in the memristor models examined except the HP and the Mutlu-Kumru memristor models. The results show that the memristor models that require infinite switching energy are not physical models despite being numerically simulatable, and, therefore, better memristor models, whose not only resistive switching time but also resistive switching energy integrals converge, are needed. In [18] to solve this problem, a new memristor model with a finite switching time has been proposed. In this study, it is also demonstrated that the Mutlu-Kumru memristor model does the resistive switching with a finite amount of energy under a DC voltage for each polarity.

The Mutlu-Kumru memristor model's switching energy is also examined parametrically. It has been shown that for high n values, the switching energy of the Mutlu-Kumru model asymptotically approaches that of the HP memristor. For the Mutlu-Kumru memristor model, it has been shown that its switching time energy is a nonlinear function of its resistive switching energy.

A memristor model must have the three fingerprints of a memristor as explained in [57]. Experimental results such as the ones given in [30, 51, 58] show that a memristor must switch in a finite time but the models examined in [18] and this study except the HP and the Mutlu-Kumru models analytically cannot do resistive switching with a finite energy in a finite time. Therefore, in [18], it is suggested that if a new memristor model is proposed in the literature, its switching time must be a finite value and the convergence of the memristor switching time integral should also be satisfied as an additional criterion besides having the three fingerprints of the memristor. In our opinion, also, the resistive switching energy of a memristor must also be finite or its switching energy integral should also converge to a finite value. Only the memristor models satisfying with the criterion given here and in [18] can be used to build memristor-based digital circuits and memories more accurately in the future.

## 6 Acknowledgments

The authors would like to thank the editors and the anonymous reviewers whose insightful comments have helped to improve the quality of this paper considerably.

## 7 References


1. L. O. Chua, "Memristor-The missing circuit element," IEEE Transactions on Circuit Theory, vol. 18, pp. 507-519, September 1971. https://doi.org/10.1109/TCT.1971.1083337.
2. L. O. Chua and S. M. Kang, "Memristive devices and systems," Proceedings of the IEEE, vol. 64, pp. 209-223, February1976. https://doi.org/10.1109/PROC.1976.10092.
3. D. B Strukov, G. S. Snider, D. R. Stewart, and R. S. Williams, "The Missing Memristor Found," Nature, vol. 453, pp. 80-83, May 2008. https://doi.org/10.1038/nature06932.
4. T. Prodromakis and C. Toumazou, "A review on memristive devices and applications," in 17th IEEE International Conference on Electronics, Circuits and Systems (ICECS), Athens, Greece, 2010, pp. 934 – 937. https://doi.org/10.1109/ICECS.2010.5724666
5. Y. V. Pershin, M. Di Ventra, "Memory effects in complex materials and nanoscale systems," Advances in Physics, vol. 60, pp. 145-227, 2011. https://doi.org/10.1080/00018732.2010.544961.
6. L. Chua, "Resistance switching memories are memristors," Applied Physics A, vol. 102, pp. 765-783, 2011. https://doi.org/10.1007/s00339-011-6264-9.
7. J. Domaradzki, D. Wojcieszak, T. Kotwica, and E. Mankowska, "Memristors: a short review on fundamentals, structures, materials and applications," International Journal of Electronics and Telecommunications, vol. 66, pp 373-381, 2020. https://doi.org/10.24425/ijet.2020.131888.
8. S. G. Hu, S. Y. Wu, W. W. Jia et al., "Review of nanostructured resistive switching memristor and its applications," Nanoscience and Nanotechnology Letters, vol. 6, pp. 729-757, 2014. https://doi.org/10.1166/nnl.2014.1888.
9. S. Shin, K. Kim, and S. M. Kang, "Memristor applications for programmable analog ICs," IEEE Transactions on Nanotechnology vol. 10, pp. 266-274, 2011. https://doi.org/10.1109/TNANO.2009.2038610.
10. T. A. Wey, W. D. Jemison, "Variable gain amplifier circuit using titanium dioxide memristors," IET Circuits, Devices & Systems, vol. 5, pp. 59-65, 2011. https://doi.org/10.1049/iet-cds.2010.0210.
11. Y. V. Pershin, M. Di Ventra, "Practical approach to programmable analog circuits with memristors," IEEE Transactions on Circuits and Systems I: Regular Papers, vol. 57, pp. 1857-1864, 2010. https://doi.org/10.1109/TCSI.2009.2038539.
12. S. C. Yener, R. Mutlu, and H. H. Kuntman, "A new memristor-based high-pass filter/amplifier: Its analytical and dynamical models," in 24th International Conference Radioelektronika, Bratislava, Slovakia, 2014, pp. 1-4. https://doi.org/10.1109/Radioelek.2014.6828420
13. A. Thomas, "Memristor-based neural networks," Journal of Physics D: Applied Physics, vol. 46, 093001, 2013. https://doi.org/10.1088/0022-3727/46/9/093001.
14. Y. N. Joglekar, S. J. Wolf, "The elusive memristor: properties of basic electrical circuits," European Journal of Physics, vol. 30, no. 4, 661, 2009. https://doi.org/10.1088/0143-0807/30/4/001.
15. Z. Biolek, D. Biolek, and V. Biolkova, "SPICE model of memristor with nonlinear dopant drift," Radioengineering, vol. 18, pp. 210-214, 2009.
16. T. Prodromakis, B. P. Peh, C. Papavassiliou, and C. Toumazou, "A versatile memristor model with nonlinear dopant kinetics," IEEE Transactions on Electron Devices, vol. 58, pp. 3099-3105, 2011. https://doi.org/10.1109/TED.2011.2158004.
17. J. Zha, H. Huang, and Y. Liu, "A novel window function for memristor model with application in programming analog circuits," IEEE Transactions on Circuits and Systems II: Express Briefs, vol. 63, pp.423-427, 2016. https://doi.org/10.1109/TCSII.2015.2505959.
18. R. Mutlu, T. D. Kumru, "A Zeno paradox: some well-known nonlinear dopant drift memristor models have infinite resistive switching time," Radioengineering, vol. 32, pp. 312-324, 2023. https://doi.org/10.13164/re.2023.0312.
19. E. Gale, "TiO2-based memristors and ReRAM: materials, mechanisms and models (a review)," Semiconductor Science and Technology, vol. 29, 104004, 2014. https://doi.org/10.1088/0268-1242/29/10/104004.
20. V. S. Baghel and S. Akashe, Low power memristor based 7T SRAM using MTCMOS technique," in 2015 Fifth International Conference on Advanced Computing & Communication Technologies, Haryana, India, 2015, pp. 222-226. https://doi.org/10.1109/ACCT.2015.58
21. J. Mohr, T. Hennen, D. Bedau et al., "Fabrication of highly resistive NiO thin films for nanoelectronic applications," Advanced Physics Research, vol. 1, 2200008, 2022. https://doi.org/10.1002/apxr.202200008
22. J. Yao, Z. Sun, L. Zhong, D. Natelson, and J. Tour, "Resistive switches and memories from Silicon Oxide," Nano Letters, vol. 10, no. 10, pp. 4105-4110, 2010. https://doi.org/10.1021/nl102255r.
23. D. H. Kwon, K. M. Kim, J. H. Jang et al., "Atomic structure of conducting nanofilaments in TiO2 resistive switching memory," Nature Nanotechnology, vol. 5, pp. 148-153, 2010. https://doi.org/10.1038/nnano.2009.456.

24. J. J. Yang, M. D. Pickett, X. Li et al., "Memristive switching mechanism for metal/oxide/metal nanodevices," Nature nanotechnology, vol. 3, pp. 429-433, 2008. https://doi.org/10.1038/nnano.2008.160.
25. H. Akinaga, H. Shima, " Resistive random access memory (ReRAM) based on metal oxidess," Proceedings of the IEEE, vol. 98, pp. 2237-2251, 2010. https://doi.org/10.1109/JPROC.2010.2070830.
26. R. Waser, M. Aono, "Nanoionics-based resistive switching memories," Nature materials, pp. 833–840 , 2007. https://doi.org/10.1038/nmat2023
27. B. J. Choi, D.S. Jeong, S. K. Kim et al., "Resistive switching mechanism of TiO2 thin films grown by atomic-layer deposition," Journal of Applied Physics, vol. 98, 033715, 2005. https://doi.org/10.1063/1.2001146.
28. H. Xie, M. Wang, P. Kurunczi; Y. Erokhin, Q. Liu, et al., " Resistive switching properties of HfO2-based ReRAM with implanted Si/Al ions," AIP Conference Proceedings, American Institute of Physics, vol. 1496, pp. 26-29, 2012. https://doi.org/10.1063/1.4766481.
29. A. A. Sivkov, Y. Xing, Z. Minden et al., "Resistive switching properties of ZrO2 film by plasma-enhanced atomic layer deposition for non-volatile memory applications," Journal of Electronic Materials, vol. 50, pp. 5396-5401, September 2021. https://doi.org/10.1007/s11664-021-09065-6.
30. E. Linn, R. Rosezin, C. Kügeler, and R. Waser, "Complementary resistive switches for passive nanocrossbar memories," Nature materials, vol. 9, pp. 403-6, 2010. https://doi.org/10.1038/nmat2748.
31. R. Rosezin, E. Linn, L. Nielen, C. Kügeler, R. Bruchhaus, and R. Waser, "Integrated complementary resistive switches for passive high-density nanocrossbar arrays," IEEE Electron Device Letters, vol. 32, pp. 191-193, 2011. https://doi.org/10.1109/LED.2010.2090127.
32. E. Karakulak, R. Mutlu, and E. Ucar, "Sneak path current equivalent circuits and reading margin analysis of complementary resistive switches based 3D stacking crossbar memories," Informacije MIDEM, vol. 44, pp. 235-241, 2014.
33. E. Karakulak, R. Mutlu, and E. Ucar, "Reconstructive sensing circuit for complementary resistive switches-based crossbar memories," Turkish Journal of Electrical Engineering & Computer Sciences, vol. 24, pp. 1371-1383, 2016. https://doi.org/10.3906/elk-1309-71.
34. L. Gao, F. Alibart, and D. B. Strukov, "Programmable CMOS/memristor threshold logic," IEEE Transactions on Nanotechnology, vol. 12, pp. 115-119, 2013. https://doi.org/10.1109/TNANO.2013.2241075.
35. C. M. Jung, K. H. Jo, E. S. Lee et al., "Zero-sleep-leakage flip-flop circuit with conditional-storing memristor retention latch," IEEE Transactions on Nanotechnology, vol. 11, pp. 360-366, 2012. https://doi.org/10.1109/TNANO.2011.2175943.
36. W. Robinett, M. Pickett, J. Borghetti et al., "A memristor-based nonvolatile latch circuit," Nanotechnology, vol. 21, 235203 2010. https://doi.org/10.1088/0957-4484/21/23/235203.
37. A. Vishwakarma, K. O. Ampadu, M. Huebner et al., "Memristor-based CMOS hybrid circuit design and analysis," Procedia Computer Science, vol. 218, pp. 563-573, 2023. https://doi.org/10.1016/j.procs.2023.01.038.
38. A. H. Edwards, H. J. Barnaby, K. A. Campbell et al., "Reconfigurable memristive device technologies," Proceedings of the IEEE, vol. 103, pp.1004-1033, 2015. https://doi.org/10.1109/JPROC.2015.2441752.
39. K. H. Jo, C. M. Jung, K.S. Min, and S. M. Kang, "Self-adaptive write circuit for low-power and variation tolerant memristors," IEEE Transactions on Nanotechnology, vol. 9, pp. 675-678, 2010. https://doi.org/10.1109/TNANO.2010.2052108.
40. I. Vourkas and G.Ch.Sirakoulis, "Emerging memristor-Based logic circuit design approaches: a review," IEEE Circuits and Systems Magazine, vol. 16, pp. 15-30, 2016. https://doi.org/10.1109/MCAS.2016.2583673.
41. F. Z. Wang, N. Helian, S. Wu et al., "Delayed switching in memristors and memristive systems," IEEE Electron Device Letters, vol. 31, pp. 755-757, 2010. https://doi.org/10.1109/LED.2010.2049560.
42. Y. Xie, "Modeling, architecture, and applications for emerging memory technologies," IEEE Design & Test of Computers, vol. 28, pp. 44-51, 2011. https://doi.org/10.1109/MDT.2011.20.
43. F. Z. Wang, N. Helian, S. Wu et al., "Delayed switching applied to memristor neural networks," Journal of Applied Physics, vol. 111, 07E317, 2012. https://doi.org/10.1063/1.3672409.
44. A. Özgüvenç, R. Mutlu, and E. Karakulak, "Sawtooth signal generator with a memristor," in 1st International Conference on Engineering Technology and Applied Sciences, Afyon, Türkiye, 2016, pp. 1-6. https://www.researchgate.net/publication/305683933_Sawtooth_signal_generator_with_a_memristor
45. S. C. Yener, R. Mutlu, T. Yener, and H. H. Kuntman, "Memristor-based timing circuit," in 2017 Electric Electronics, Computer Science, Biomedical Engineerings' Meeting (EBBT), İstanbul, Türkiye, 2017, pp. 1–3. https://doi.org/10.1109/EBBT.2017.7956776
46. R. Mutlu and E. Karakulak, "A methodology for memristance calculation," Turkish Journal of Elec-

trical Engineering & Computer Sciences, vol. 22, pp. 121-131, 2014. https://doi.org/10.3906/elk-1205-16.
47. K. M. Kim, J. Zhang, C. Graves et al., "Low-power, self-rectifying, and forming-free memristor with an asymmetric programing voltage for a high-density crossbar application," Nano Letters, vol. 16, pp. 6724–6732, 2016. https://doi.org/10.1021/acs.nanolett.6b01781.
48. D. Niu, Y. Chen, and Y. Xie, "Low-power dual element memristor based memory design," in Proceedings of the 16th ACM/IEEE international symposium on Low power electronics and design, Austin, Texas, USA, 2010, pp. 25-30. https://doi.org/10.1145/1840845.1840851.
49. X. Guo, E. Ipek, and T. Soyata, "Resistive computation: Avoiding the power wall with low-leakage, STT-MRAM based computing," ACM SIGARCH computer architecture news, vol.38, pp. 371-382, 2010. https://doi.org/10.1145/1816038.1816012.
50. R. Mutlu, "AC power formula for unsaturated TiO2 memristors with linear dopant drift, small signal AC power formula for all memristors, and some applications for these formulas," European J. Eng. App. Sci. (EJEAS), vol. 1 , pp. 51 - 58, 2018.
51. M. E. Fouda, A. G. Radwan, "Power dissipation of memristor-based relaxation oscillators," Radioengineering, vol. 24, pp. 968-973, 2015. https://doi.org/10.13164/re.2015.0968.
52. S. Gazabare, R J. Pieper, W. Wondmagegn, and N. Satyala, "Observations on model based predictions for memristor power dissipation," in 2011 Proceedings of IEEE Southeastcon, pp. 450-454, 2011. https://doi.org/10.1109/SECON.2011.5752984.
53. Y. Ho, G. M. Huang, and P. Li, "Dynamical properties and design analysis for nonvolatile memristor memories," IEEE Transactions on Circuits and Systems I: Regular Papers, vol. 58, pp.724-736, 2011. https://doi.org/10.1109/TCSI.2010.2078710.
54. S. Vongehr, X. Meng, " The missing memristor has not been found," Scientific Reports, vol. 5, 11657, 2015. https://doi.org/10.1038/srep11657.
55. K. Soni, S. Sahoo, "A review on different memristor modeling and applications," in 2022 International Mobile and Embedded Technology Conference (MECON), Noida, India, 2022, pp. 688-695. https://doi.org/10.1109/MECON53876.2022.9752214.
56. Zeno's paradoxes, https://en.wikipedia.org/wiki/Zeno%27s_paradoxes [accessed on February 17, 2023].
57. S.P. Adhikari, M. P. Sah, H. Kim, and L. O. Chua, "Three fingerprints of memristor," IEEE Transactions on Circuits and Systems I: Regular Papers, vol. 60, pp. 3008-3021, 2013. https://doi.org/10.1109/TCSI.2013.2256171.
58. J. Mustafa, R. Waser, "A novel reference scheme for reading passive resistive crossbar memories," IEEE Transactions on Nanotechnology, vol. 5, pp. 687-691, 2006. https://doi.org/10.1109/TNANO.2006.885016.



Arrived: 05. 12. 2023
Accepted: 29. 02. 2024